J|A|C|S ARTICLES

Published on Web 05/04/2010

Para-hydrogenated Glucose Derivatives as Potential ^{13}C-Hyperpolarized Probes for Magnetic Resonance Imaging

Francesca Reineri,[†] Daniela Santelia,[†] Alessandra Viale,[†] Erika Cerutti,[†] Luisa Poggi,[‡] Tomas Tichy,[§] Samuel S. D. Premkumar,[†] Roberto Gobetto,[†] and Silvio Aime*,[†]

Dipartimento di Chimica IFM, University of Torino, Via P. Giuria 7, 10125 Torino, Italy, Bracco Imaging S.p.A., Via Ribes 5, 10010 Colleretto Giacosa (TO), Italy, and Institute of Organic Chemistry and Biochemistry, Academy of Sciences of the Czech Republic, Flemingovo nam. 2, 166 10, Prague 6, Czech Republic

Received February 17, 2010; E-mail: silvio.aime@unito.it

Abstract: A set of molecules in which a glucose moiety is bound to a hydrogenable synthon has been synthesized and evaluated for hydrogenation reactions and for the corresponding para-hydrogen-induced polarization (PHIP) effects, in order to select suitable candidates for an *in vivo* magnetic resonance imaging (MRI) method for the assessment of glucose cellular uptake. It has been found that amidic derivatives do not yield any polarization enhancement, probably due to singlet−triplet state mixing along the reaction pathway. In contrast, ester derivatives are hydrogenated in high yield and afford enhanced ^{1}H and ^{13}C NMR spectra after para-hydrogenation. The obtained PHIP patterns are discussed and explained on the basis of the calculated spin level populations in the para-hydrogenated products. These molecules may find interesting applications in ^{13}C MRI as hyperpolarized probes for assessing the activity of glucose transporters in cells.

Introduction

Much attention has been devoted in recent years to the development of hyperpolarized ^{13}C contrast agents for ^{13}C magnetic resonance imaging (MRI).[1−16] Two methodologies are currently available for the production of ^{13}C-hyperpolarized molecules, namely dynamic nuclear polarization (DNP)[3−6,15−21] and para-hydrogen-induced polarization (PHIP).[1,7−14,22−35]

[†] University of Torino.
[‡] Bracco Imaging S.p.A.
[§] Academy of Sciences of the Czech Republic.

(1) Golman, K.; Axelsson, O.; Johannesson, H.; Mansson, S.; Olofsson, C.; Petersson, J. S. *Magn. Reson. Med.* **2001**, *46*, 1.
(2) Mansson, S.; Johansson, E.; Magnusson, P.; Chai, C. M.; Hansson, G.; Petersson, J. S.; Stahlberg, F.; Golman, K. *Eur. Radiol.* **2006**, *16*, 57, and references therein.
(3) Golman, K.; Petersson, J. S. *Acad. Radiol.* **2006**, *13*, 932, and references therein.
(4) Golman, K.; Zandt, R.; Thaning, M. *Proc. Natl. Acad. Sci. U.S.A.* **2006**, *103*, 11270.
(5) Golman, K.; Zandt, R.; Lerche, M.; Perhson, R.; Ardenkjaer-Larsen, H. *Cancer Res.* **2006**, *66*, 10855.
(6) Kohler, S. J.; Yen, Y.; Wolber, J.; Chen, A. P.; Albers, M. J.; Bok, R.; Zhang, V.; Trop, J.; Nelson, S.; Vigneron, D. B.; Kurhanewicz, J.; Hurd, R. E. *Magn. Reson. Med.* **2007**, *58*, 65.
(7) Bhattacharya, P.; Chekmenev, E. Y.; Perman, W. H.; Harris, K. C.; Lin, A. P.; Norton, V. A.; Tan, C. T.; Ross, B. D.; Weitekamp, D. P. *J. Magn. Reson.* **2007**, *186*, 150.
(8) Ishii, M.; Emami, K.; Kadlecek, S.; Petersson, J. S.; Golman, K.; Vahdat, V.; Yu, J.; Cadman, R. V.; MacDuffie-Woodburn, J.; Stephen, M.; Lipson, D. A.; Rizi, R. R. *Magn. Reson. Med.* **2007**, *57*, 459.
(9) Magnusson, P.; Johansson, E.; Mansson, S.; Petersson, J. S.; Chai, C. M.; Hansson, G.; Axelsson, O.; Golman, K. *Magn. Reson. Med.* **2007**, *57*, 1140.
(10) Goldman, M.; Johannesson, H.; Axelsson, O.; Karlsson, M. *Magn. Reson. Imag.* **2005**, *23*, 153.
(11) Johannesson, H.; Axelsson, O.; Karlsson, M. *C. R. Phys* **2004**, *5*, 315.
(12) Goldman, M.; Johannesson, H. *C. R. Phys.* **2005**, *6*, 575.
(13) Johansson, E.; Olsson, L. E.; Mansson, S.; Petersson, J. S.; Golman, K.; Stahlberg, F.; Wirestam, R. *Magn. Reson. Med.* **2004**, *52*, 1043.
(14) Golman, K.; Olsson, L. E.; Axelsson, O.; Mansson, S.; Karlsson, M.; Petersson, J. S. *Br. J. Radiol.* **2003**, *76*, S118.
(15) Svensson, J.; Mansson, S.; Johansson, E.; Petersson, J. S.; Olsson, L. E. *Magn. Reson. Med.* **2003**, *50*, 256.
(16) Golman, K.; Ardenkjaer-Larsen, J. H.; Petersson, J. S.; Mansson, S.; Leunbach, I. *Proc. Natl. Acad. Sci. U.S.A.* **2003**, *100*, 10435.
(17) Abragam, A.; Goldman, M. *Rep. Prog. Phys.* **1978**, *41*, 395.
(18) Ardenkjaer-Larsen, J. H.; Fridlund, B.; Gram, A.; Hansson, G.; Hansson, L.; Lerche, M. H.; Servin, R.; Thaning, M.; Golman, K. *Proc. Natl. Acad. Sci. U.S.A.* **2003**, *100*, 10158.
(19) Hall, D. A.; Maus, D. C.; Gerfen, G. J.; Inati, S. J.; Becerra, L. R.; Dahlquist, F. W.; Griffin, R. G. *Science* **1997**, *276*, 930.
(20) Gerfen, G. J.; Becerra, L. R.; Hall, D. A.; Griffin, R. G.; Temkin, R. J.; Singel, D. J. *J. Chem. Phys.* **1995**, *102*, 9494.
(21) Un, S.; Prisner, T.; Weber, R. T.; Seaman, M. J.; Fishbein, K. W.; McDermott, A. E.; Singel, D. J.; Griffin, R. G. *Chem. Phys. Lett.* **1992**, *189*, 54.
(22) Eisenberg, R. *Acc. Chem. Res.* **1991**, *24*, 110, and references therein.
(23) Natterer, J.; Bargon, J. *Prog. Nucl. Magn. Reson. Spectrosc.* **1997**, *31*, 293, and references therein.
(24) Duckett, S. B.; Sleigh, C. J. *Prog. Nucl. Magn. Reson. Spectrosc.* **1999**, *34*, 71, and references therein.
(25) Bowers, C. R.; Weitekamp, D. P. *Phys. Rev. Lett.* **1986**, *57*, 2645.
(26) Pravica, M. G.; Weitekamp, D. P. *Chem. Phys. Lett.* **1988**, *145*, 255.
(27) Natterer, J.; Schedletzky, O.; Barkemeyer, J.; Bargon, J. *J. Magn. Reson.* **1998**, *133*, 92.
(28) Stephan, M.; Kohlman, O.; Niessen, H. G.; Eichhorn, A.; Bargon, J. *Magn. Reson. Chem.* **2002**, *40*, 157.
(29) Barkemeyer, J.; Haake, M.; Bargon, J. *J. Am. Chem. Soc.* **1995**, *117*, 2927.
(30) Haake, M.; Barkemeyer, U.; Bargon, J. *J. Phys. Chem.* **1995**, *99*, 17539.
(31) Bargon, J.; Bommerich, U.; Kadlecek, S.; Ishii, M.; Fischer, M. C.; Rizi, R. R. *Proc. Int. Soc. Magn. Reson. Med.* **2005**, *13*, 2572.
(32) Barkemeyer, J.; Haake, M.; Bargon, J. *J. Am. Chem. Soc.* **1995**, *117*, 2727.

 10.1021/ja101399q

When compared to DNP, the PHIP approach appears definitely cheaper and more easily applicable, as it does not require the very low temperatures needed in the DNP method. However, the major advantage of DNP is that, in principle, it can be applied to hyperpolarize any molecule, while the PHIP procedure has specific structural requirements for the substrates to be hyperpolarized. In fact, the PHIP-based procedure consists of the catalytic para-hydrogenation of an unsaturated molecule, followed by the removal of both the catalyst and the organic solvent from the reaction mixture before injection. The transformation of para-hydrogen spin order into net heteronuclear hyperpolarization may be achieved either by a field cycling procedure[35] or through the application of a suitable pulse sequence.[12] The first step toward an *in vivo* application of the PHIP procedure involves the search for unsaturated substrates, which must be efficiently hydrogenated to yield water-soluble products. Furthermore, these molecules must contain a ^{13}C nucleus characterized by a long relaxation time (carbonyl or quaternary carbon atom), scalarly coupled with the para-hydrogen atoms.

Until now, only the following few molecules have been considered for the development of ^{13}C-hyperpolarized MRI applications: 2-hydroxyethyl propionate (derived from hydrogenation of 2-hydroxyethyl acrylate),[10−14] succinic acid (obtained by hydrogenation of fumaric acid), methyl 2-butenoate (obtained by hydrogenation of methyl 2-butynoate), and bis[2-(2-methoxyethoxy)ethyl] maleate (derived from hydrogenation of bis[2-(2-methoxyethoxy)ethyl]acetylene dicarboxylate). The latter system has been used as a model for the setup of a fast procedure to eliminate the catalyst and the organic solvent, based on a phase-transfer process.[34]

The most challenging application of ^{13}C-hyperpolarized molecules deals with their use as metabolic imaging reporters. The prototype of these probes is represented by DNP-hyperpolarized pyruvate, which *in vivo* transforms into alanine, lactate, and bicarbonate. The increased metabolic activity of tumor cells has been assessed on animal models by quantifying the relative amounts, at the cellular level, of the products of pyruvate metabolism.[6,36,37]

Until now, in clinical practice, the most important *in vivo* metabolic imaging assay has been represented by the positron emission tomography (PET) measure of glucose uptake. A ^{18}F surrogate of glucose (fluorodesoxyglucose, FDG), which accumulates in tumor cells showing an up-regulation of glucose transporters, is currently used. We wonder whether a ^{13}C-hyperpolarized glucose derivative could be considered as a viable MRI alternative to the complex and expensive FDG/PET procedure.

As a hydrogenation route to glucose cannot be easily envisaged, we have synthesized a set of molecules in which the sugar moiety is bound to a hydrogenable synthon. The work reported herein deals with the evaluation of the hydrogenation reactions and the corresponding PHIP effects on this set of molecules, in order to select suitable candidates for an *in vivo* MRI method for the assessment of glucose cellular uptake.

Results and Discussion

The new substrates synthesized in this work and tested for para-hydrogenation are shown in Chart 1. The unsaturated moiety is represented in most cases by a butynoic acid residue and in one case by propiolic acid.

The glucosamine derivatives of butynoic acid, 2-(but-2-ynylamido)-2-deoxy-α,*β*-D-glucopyranose (**1**) and 1,3,4,6-tetra-*O*-acetyl-2-(but-2-ynylamido)-2-deoxy-α,*β*-D-glucopyranose (**2**), were obtained by reaction of acetyl-protected glucosamine with butynoyl chloride and, in the case of **1**, successive deacetylation in sodium methanolate−methanol (Scheme 1). The propiolic acid derivative 2-(propiolamido)-2-deoxy-α,*β*-D-glucopyranose (**3**) was obtained by the same procedure, using 3-(trimethylsilyl)propynoic acid in place of 2-butynoic acid (in order to avoid acylation reaction employing very unstable propynoic acid chloride), and successive desilylation and deacetylation by reaction with K_2CO_3 in anhydrous methanol. Dissolution of the product in deuterated water or methanol promoted the deuteration of all the exchangeable protons in the molecule (including the alkynic one), affording the corresponding perdeuterated derivative (**3D**).

Ester derivatives of glucose 6-*O*-(but-2-ynoyl)-α,*β*-D-glucopyranose (**4**) and 2-*O*-(but-2-ynoyl)-α,*β*-D-glucopyranose (**5**) were obtained by reacting butynoyl chloride and glucose in dimethylformamide (DMF) in the presence of K_2CO_3 (Scheme 2). Separation of the two isomers was achieved by column chromatography. Higher yields can be obtained by using acetylated glucose, but during the following deacetylation step the just-formed ester bond is readily cleaved.

1-*O*-(But-2-ynoyl)-α,*β*-D-glucopyranose (**6**) and 1-*O*-[2-(but-2-ynoyl)ethyl]-α,*β*-D-glucopyranose (**7**) were obtained by the reaction of glucose and 1-*O*-(D-glucopyranosyl)ethylene glycol, respectively, with butynoic acid under Mitsunobu conditions[38] (Schemes 3 and 4). In the first case a mixture of **5** and **6** was formed, and the two isomers were separated by column chromatography.

The products were characterized by mass spectrometry and NMR spectroscopy. In particular, the occurrence of the covalent linkage between the glucose moiety and the alkyne was assessed by means of heteronuclear multiple-bond correlation (HMBC) experiments, showing in all cases a well-defined cross peak between the carbonyl carbon atom of the alkyne and the H-2 (for **1**, **2**, **3**, and **5**), H-6 (for **4**), H-1 (for **6**), or H-8 (for **7**) proton resonances of the ring. In **7** the cross-peak between H-1 and H-7 was also observed. A complete assignment of the ^1H and ^{13}C NMR data, obtained by means of heteronuclear multiple-quantum coherence (HMQC) and distortionless enhancement by polarization transfer (DEPT) experiments, further confirmed the proposed structures.

With the exception of **3**, mass spectra did not show molecular peaks. Instead, peaks corresponding to species derived from the progressive loss of water from the original protonated com-

(33) Chekmenev, E. Y.; Hövener, J.; Norton, V. A.; Harris, K.; Batchelder, L. S.; Bhattacharya, P.; Ross, B. D.; Weitekamp, D. P. *J. Am. Chem. Soc.* **2008**, *130*, 4212.
(34) Reineri, F.; Viale, A.; Giovenzana, G.; Santelia, D.; Dastrù, W.; Gobetto, R.; Aime, S. *J. Am. Chem. Soc.* **2008**, *130*, 15047.
(35) Jóhannesson, H.; Axelsson, O.; Karlsson, M. *C. R. Phys.* **2004**, *5*, 315.
(36) Nelson, S. J.; Vigneron, D.; Kurhanewicz, J.; Chen, A.; Bok, R.; Hurd, R. *Appl. Magn. Reson.* **2008**, *34*, 533.
(37) Albers, M. J.; Bok, R.; Chen, A. P.; Cunningham, C. H.; Zierhut, M. L.; Yi Zhang, V.; Kohler, S. J.; Tropp, J.; Hurd, R. E.; Yen, Y.; Nelson, S. J.; Vigneron, D. B.; Kurhanewicz, J. *Cancer Res.* **2008**, *68*, 8607.
(38) Bottle, S.; Jenkins, I. D. *J. Chem. Soc., Chem. Commun.* **1984**, 385.

Chart 1. Synthesized Glucose Derivatives

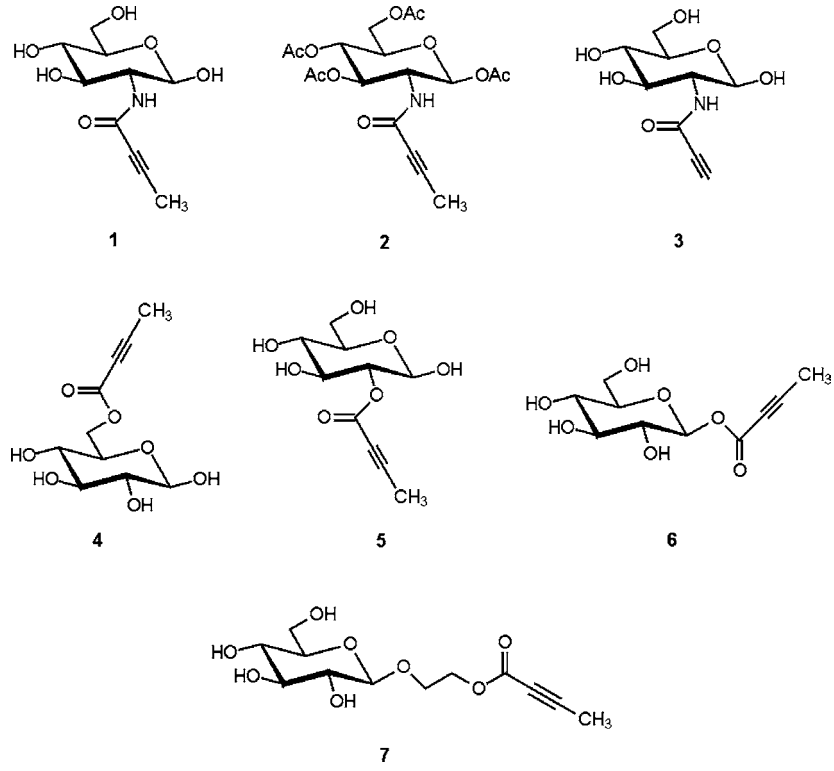

Scheme 1. Reaction Scheme for the Synthesis of **1**, **2**, and **3**

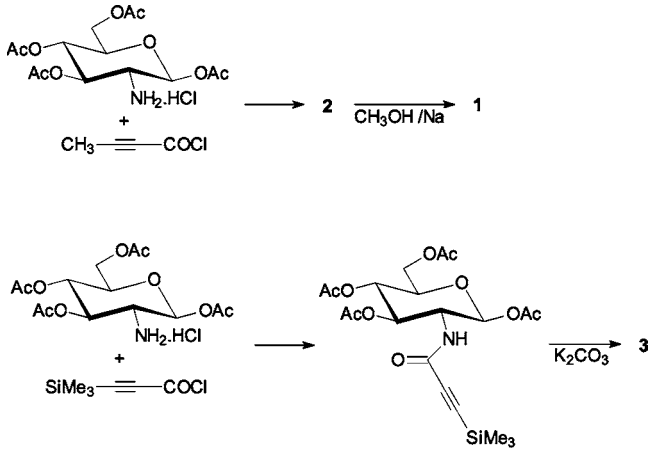

Scheme 2. Reaction Scheme for the Synthesis of **4** and **5**

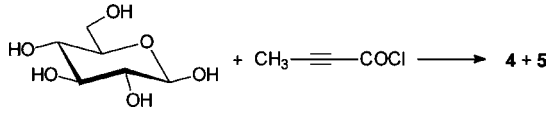

Scheme 3. Reaction Scheme for the Synthesis of **6**

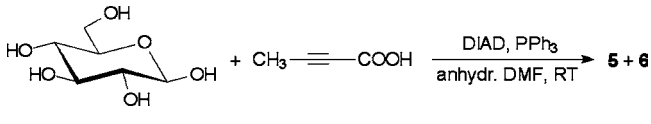

pounds (MW + H^+ − H_2O = MW-17; MW + H^+ − $2H_2O$ = MW-35, etc.) and an additional peak corresponding to the addition of sodium (MW + 23) were detected. The same behavior was observed in the corresponding mass spectra of the parent glucose and glucosamine. The acetylated derivative **2** showed a similar behavior, as the highest intensity peak in its mass spectrum corresponds to the loss of one acetyl group from the protonated compound (MW + H^+ − $OCOCH_3$ = MW-60).

In methanol solutions the α anomers were predominant ($\alpha/\beta = 3-10$) for **1**, **2**, **3**, and **7**, in analogy to what was observed in the case of D-glucose, while for **4**, **5**, and **6** there was a slight prevalence of the β anomers ($\alpha/\beta = 0.8$ for **4** and 0.7 for **5** and **6**).

Para-hydrogenation reactions were carried out in a 5 mm NMR tube equipped with a Young valve, using [Rh(COD)(dppb)][BF_4] as catalyst, in acetone-d_6/CD_3OD 9:1 solutions (see Experimental Section for details). Although lower hydrogenation yields are observed in the presence of methanol with respect to pure acetone solutions, the use of methanol was necessary to completely dissolve the compounds.

The amidic derivative of glucose and 2-butynoic acid (**1**) could not be hydrogenated at all under the experimental conditions used in this work. The corresponding peracetyl derivative (**2**) was tested in pure acetone in order to maintain a higher catalytic efficiency, but also in this case the hydrogenation yield was negligible.

In contrast, the amidic derivative of glucose and propiolic acid (**3**) was hydrogenated in quite high yield (60%, Scheme 5), thanks to the lower steric hindrance around the unsaturation that allows better interaction with the Rh atom. Nevertheless, when para-hydrogen was used, the olefinic protons showed only slightly enhanced adsorption/emission ^{1}H NMR signals (5.72, 6.51, and 6.33 ppm for Ha, Hb, and Hc, respectively, Figure 1) derived from longitudinal spin order $I_z^{Ha}I_z^{Hb}$, instead of the longitudinal magnetization terms ($I_z^{Ha} - I_z^{Hb}$) which are usually obtained when ALTADENA experiments are carried out. Furthermore, no polarization was detected in the ^{13}C NMR spectrum, not even when the analogous perdeuterated derivative

Scheme 4. Reaction Scheme for the Synthesis of **7**

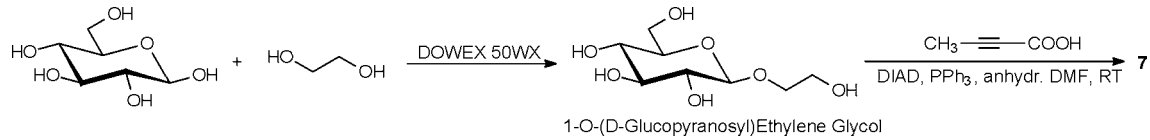

Scheme 5. Hydrogenation of Glucosamine Derivatives

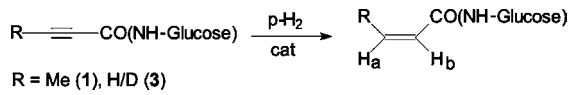

was used. The lack of ^{13}C polarization, in spite of the high hydrogenation efficiency, might be related to the loss of the zero quantum coherence term of para-hydrogen ($I_x^{Ha}I_x^{Hb} + I_y^{Ha}I_y^{Hb}$) due to the singlet/triplet mixing that can occur along the reaction pathway.[39] This view is supported by the fact that also longitudinal magnetization, which is usually observed in ALTADENA experiments, derives from the zero quantum coherence term, while in this case only antiphase signals corresponding to $I_z^{Ha}I_z^{Hb}$ are obtained.

Unlike amide derivatives, para-hydrogenation of unsaturated esters (Scheme 6) leads to hyperpolarized in-phase signals that are typical of ALTADENA experiments: this means that zero quantum coherence is retained in the para-hydrogenation reactions of **4**−**7**.

4−**7** showed excellent hydrogenation rates, resulting in 100% yields and PHIP effects much higher than those observed in the case of amide derivatives. In Figure 2 the ^1H spectrum relative to compound **4** is reported. The PHIP pattern and the enhancement for **5**−**7** are analogous to those of **4**. Enhancement involves one of the two olefinic protons (Ha, 6.27 ppm) and the methyl protons (1.99 ppm), while Hb (5.65 ppm) is only slightly polarized. The observed behavior can be accounted for in terms of the spin level populations of the para-hydrogenated molecule.

Let us consider the spin system formed by the two olefinic protons (para-hydrogen protons, Ha and Hb) and, for simplicity, only one methyl proton (the effect of considering three distinct protons would be a splitting of each level into three, without changing the overall energy diagram). As the hydrogenation reaction takes place outside the spectrometer (ALTADENA experiment), all protons resonate at the same Larmor frequency, and the strong coupling condition among them is achieved, as described by the *J*-coupling Hamiltonian:

$$H_J = J_{ab}\left(I_z^aI_z^b + \frac{1}{2}(I_+^aI_-^b + I_+^bI_-^a)\right) + J_{a3}\left(I_z^aI_z^3 + \frac{1}{2}(I_+^aI_-^3 + I_+^3I_-^a)\right) + J_{b3}\left(I_z^bI_z^3 + \frac{1}{2}(I_+^bI_-^3 + I_+^3I_-^b)\right)$$

As a consequence, the spin states of all three protons are mixed, as follows:

$$\Psi_1 = |\alpha\alpha\alpha\rangle$$

$$\Psi_{2,3,4} = c_1^{2,3,4}|\alpha\alpha\beta\rangle + c_2^{2,3,4}\frac{1}{\sqrt{2}}|\alpha\beta + \beta\alpha\rangle|\alpha\rangle + c_3^{2,3,4}\frac{1}{\sqrt{2}}|\alpha\beta - \beta\alpha\rangle|\alpha\rangle$$

$$\Psi_{5,6,7} = c_1^{5,6,7}|\beta\beta\alpha\rangle + c_2^{5,6,7}\frac{1}{\sqrt{2}}|\alpha\beta + \beta\alpha\rangle|\beta\rangle + c_3^{5,6,7}\frac{1}{\sqrt{2}}|\alpha\beta - \beta\alpha\rangle|\beta\rangle$$

$$\Psi_8 = |\beta\beta\beta\rangle$$

where the coefficients are the eigenvectors of the Hamiltonian matrix written using the reported spin states as the basis set.[40]

The population of each level is a function of the para-hydrogen contribution to that state. From numerical calculation (results summarized in Table 1)[40] it is found that overpopulation derived from para-hydrogen is concentrated in the lowest energy spin states, having $M_z = 1/2$ and $M_z = -1/2$, respectively (these levels are indicated by thicker lines in Figure 3). The adiabatic transfer of the sample into the spectrometer maintains the same spin states population pattern. As shown in Figure 3, the enhanced transitions involve the methyl proton (H_3, emission) and Ha (adsorption), while the Hb transition occurs between levels that are almost equally populated, thus resulting in no signal enhancement.

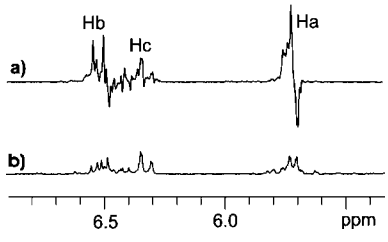

Figure 1. Single-scan ^1H NMR spectra (acetone-d_6/CD_3OD 9:1, 298 K, 9.4 T, olefinic region) recorded (a) immediately after para-hydrogenation of **3** and (b) after relaxation (60 s).

Scheme 6. Hydrogenation of Glucose-2-butynoic Acid Derivatives

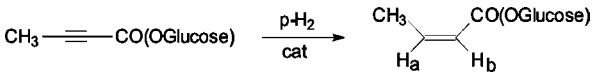

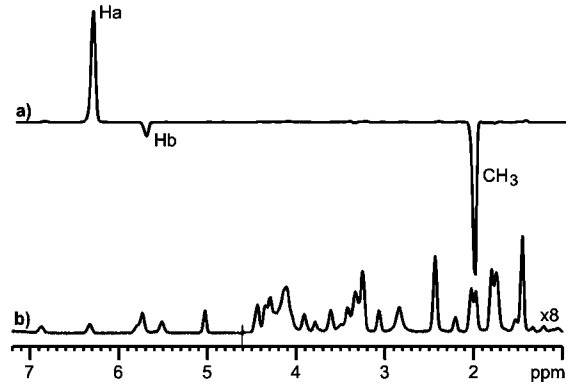

Figure 2. Single-scan ^1H NMR spectrum (acetone-d_6/CD_3OD 9:1, 298 K, 9.4 T) recorded immediately after para-hydrogenation of **4**.

Table 1

	E (Hz)	$c_1^{2,3,4}$	$c_2^{2,3,4}$	$c_3^{2,3,4}$
Ψ_2	-1.0086×10^3	0.1693	0.0607	**−0.9837**
Ψ_3	-1.0017×10^3	0.7944	−0.5991	0.0997
Ψ_4	-0.9947×10^3	−0.5833	−0.7984	−0.1496

	E (Hz)	$c_1^{5,6,7}$	$c_2^{5,6,7}$	$c_3^{5,6,7}$
Ψ_5	0.9911×10^3	0.2365	−0.1672	**−0.9571**
Ψ_6	0.9989×10^3	−0.7815	0.5526	−0.2896
Ψ_7	1.0050×10^3	0.5774	0.8165	0.0

In Figure 4 the ^{13}C NMR spectra recorded after para-hydrogenation of **4** are reported. Analogous results were obtained for **5**−**7**.

When the spectrum is recorded immediately after the para-hydrogenation reaction (Figure 4a), polarization is observed only on the methyl signal (14.47 ppm), while the carbonyl ^{13}C nucleus, which is also scalarly coupled with para-hydrogen protons, does not show any enhancement. This is due to the fact that polarization on the ^{13}C methyl signal derives from the strongly polarized methyl protons rather than from the olefinic ones, as confirmed by using the analogous deuterated compound. A more detailed explanation is beyond the scope of this work.

The spectrum shown in Figure 4b was recorded after the application of a field-cycling procedure to the para-hydrogenated sample. It consists of two asymmetric transformations of the magnetic field: in the first passage the sample is quickly (non-adiabatically) thrown from 50 μT (Earth's field) to a nearly zero (0.1 μT) magnetic field, and then it is slowly (adiabatically) brought back to the Earth's magnetic field.[35] The zero-field condition matches ^{1}H and ^{13}C Larmor frequencies (the calculated resonance frequencies of ^{1}H and ^{13}C are respectively 4.3 and 1.1 Hz at 0.1 μT); in other words, the isotropic mixing condition between heteronuclei is achieved. This leads to a change in the spin level populations, and a net enhanced emission carbonyl signal can be detected at 165.68 ppm (signal enhancement of about 350).

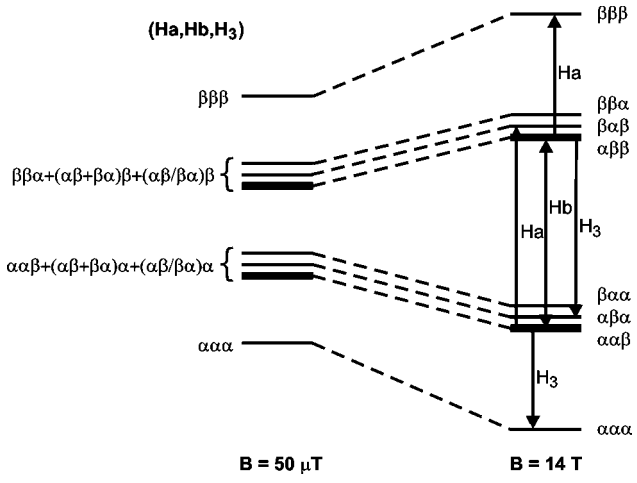

Figure 3. Schematic representation of the nuclear spin levels and allowed enhanced transitions in para-hydrogenated **4**−**7**.

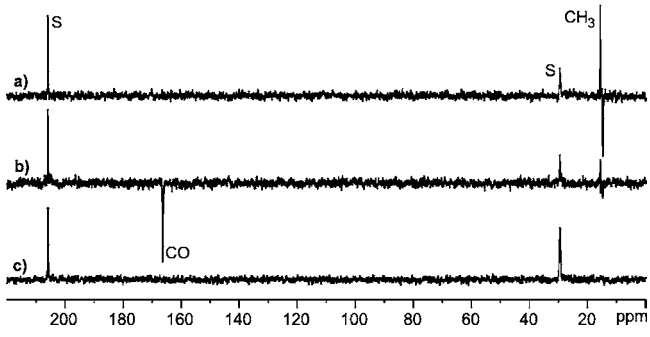

Figure 4. Single-scan ^{13}C NMR spectra (acetone-d_6/CD_3OD 9:1, 298 K, 14.0 T) recorded (a) immediately after para-hydrogenation of **4**, (b) immediately after para-hydrogenation of **4** and application of the field-cycling procedure, and (c) after relaxation (60 s, the relaxed spectrum is identical in the two experiments). S indicates the solvent peaks.

On the basis of the obtained results, **4**−**7** appear promising candidates for the setup of an HP-MRI method to assess the glucose cellular uptake. Therefore, we measured the longitudinal relaxation times of their ^{13}C carbonyl resonances. T_1 values of 10.2 and 9.3 s were obtained at 9.37 T in pure degassed CD_3OD solutions for hydrogenated **4** (**4a**) and **6** (**6a**), respectively. Even considering that the chemical shift anisotropy contribution to relaxation would be decreased at lower field, relaxation in these compounds appears to be too fast to allow further manipulations after para-hydrogenation without conspicuous polarization losses. For hydrogenated **5** (**5a**), T_1 has not been measured, but it is expected to be quite similar to that of **6a** on the basis of the similar molecular structure. It was therefore deemed useful to insert an ethyloxy spacer between the glucose ring and the alkyne (compound **7**), in order to give more rotational freedom to the unsaturated synthon. This modification yielded a significant lengthening of the carbonyl T_1 in the corresponding alkene (**7a**) with respect to **6a**. In fact, the measured T_1 value for hydrogenated **7** (**7a**) in the same experimental conditions as for **6a** is 21.0 s, which makes this molecule a suitable candidate for further MRI investigations.

Thus, **7a** was chosen as the substrate for uptake experiments on cells, in order to assess whether substitution in the 1-position of the glucose ring affects its transport through the cell membrane. A toxicity test was carried out on the K562 (human myelogenous leukemia) cell line. Cell viability, measured by the trypan blue exclusion test,[41] was found to be >95%, even when the concentration of **7a** was increased to 100 mM for 4 h of uptake time.

7a was therefore used for uptake measurements, showing a good level of internalization even at low incubation times. A 100 mM sample of **7a** was incubated in a culture of K562 cells for 1, 5, 10, 60, and 240 min at 37 °C. The occurrence of simple substrate binding at the cell membrane was ruled out by carrying out the incubation at 4 °C. NMR spectra recorded in the presence of an internal standard (see Experimental Section) allowed a quantitative determination of the number of **7a** molecules taken up by each cell at different incubation times. The obtained results are shown in Figure 5. Despite the very low S/N ratio of NMR spectra recorded after 1 and 5 min of uptake, it appears evident that the compound is indeed internalized even at very short time. Moreover, it seems that after 240 min a saturation plateau is reached. Thus, one may conclude that **7a** is internalized by the glucose transporters and can be accumulated in the cell over time.

(39) Kating, P.; Wandelt, A.; Selke, R.; Bargon, J. *J. Phys. Chem.* **1993**, *97*, 13313.
(40) The spin functions coefficients were calculated using $\nu_L = 2000$ Hz, $J_{ab} = 11$ Hz, $J_{a3} = 7$ Hz, $J_{b3} = 2$ Hz.
(41) Strober W. Trypan blue exclusion test of cell viability. *Current Protocols in Immunology*; Wiley: New York, May 2001; Appendix 3B.

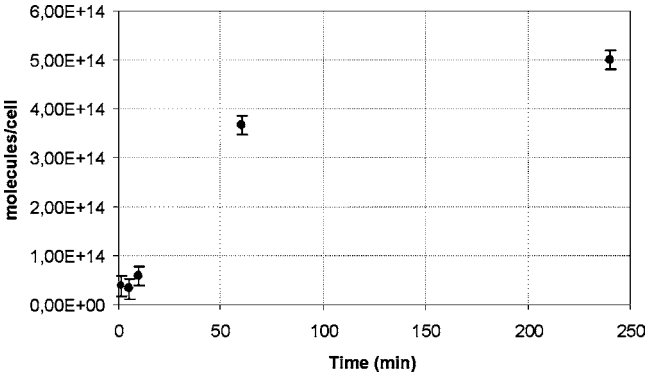

Figure 5. Uptake of 100 mM **7a** in the K562 cells.

Although the origin and mechanism of the enhanced glycolysis in cancers is still under investigation, evidence exists that it reflects the up-regulation of glucose transporters in human malignancies, enhancing glucose influx into the proliferating cancer cells.[42] Recent studies have shown that, for cancer cells, the Michaelis−Menten constant (K_M) for the glucose transporter GLUT-1, which is overexpressed in tumors, is around 10 mM.[43] Data on the uptake of glucose by K562 cells (100 mM, 1 min) show that the concentration of internalized glucose per cell is 15-fold higher than that obtained for derivative **7a**. We can assume that this difference in uptake is related to changes in enzyme−substrate affinity, i.e., in K_M in the Michaelis−Menten equation, leaving V_{max} unaffected. We can therefore estimate the K_M value for **7a**, which is about 0.7 mM. Harris et al. obtained $K_M = 2.14$ mM for pyruvate internalization in cancer cells.[44] Comparing this value with our results, we expect the internalized concentration of **7a** to be about one-third lower than the value obtained for pyruvate at any time point of the uptake curve. Furthermore, this concentration is higher than that measured by Harris et al. for lactate in the same set of experiments, and thus we believe it would be sufficiently high to allow detection of hyperpolarized **7a** within the lifetime of its ^{13}C polarization.

7a will thus be considered for further studies aimed at assessing its activity as a reporter of glucose transporters *in vivo*. The problem, when going to the hyperpolarized experiments *in vivo*, will be the distinction between the intra- and extracellular substrate molecules since there is no phosphorylation and thus no change in chemical shift. One possibility to tackle this issue may be the use of paramagnetic contrast agents (such as Gd complexes) which, being designed to not cross the cellular membrane, may "quench" the polarization in the extracellular/intravascular space but not in the intracellular one.[45,46]

Next we investigated the potential of **7a** to act as a reporter of the enzymatic phosphorylation which glucose undergoes upon cellular internalization. As expected for glucose derivatives substituted at the 1-position, **7a** did not show any phosphorylation when used in the enzymatic glucose assay. Substitution of glucose at the 2-position would overcome this problem since it does not preclude interaction with the enzyme and subsequent transformation. Therefore, a phosphorylation assay was carried out on **5a** in order to verify the hypothesis. The enzymatic assay showed that phosphorylation and subsequent oxidation of **5a** take place, as expected. Furthermore, the ^{13}C NMR spectrum of the product showed a carbonyl chemical shift difference between the starting **5a** and the final phosphorylated and oxidized product of about 0.6 ppm. This value appears at the limit for the desired applications of **7a** as probe for metabolic imaging based on the acquisition of chemical shift imaging protocols. Furthermore, it appears necessary to introduce a spacer between the alkyne and the glucose moieties (as done on going from **6** to **7**) in order to lengthen the T_1 of the ^{13}C carbonyl resonance. This structural modification is expected to further decrease the chemical shift difference between the ^{13}C carbonyl resonances in the hydrogenated product and its phosphorylated/oxidized derivatives. Thus, one may conclude that even a glucose derivatized at the 2-position would not be suitable for metabolic imaging.

Conclusions

The results reported herein establish that the presence of the amide functionality affects negatively both the hydrogenation process and the attainment of polarization effects in the NMR spectra of para-hydrogenated glucosamine olefinic derivatives.

Conversely, the ester derivatives **4**−**6**, in which 2-butynoic acid is bound to the 6-, 2-, and 1- position of the glucose ring, respectively, and **7**, in which a short ethyleneglycol spacer is inserted between the butynoic moiety and the 1-position of the ring, showed excellent para-hydrogenation yields and displayed high ^{13}C enhancement for the methyl resonance, and for the carbonyl signal after application of a field-cycling procedure. T_1 measurements showed that hydrogenated **4**−**6** are characterized by carbonyl ^{13}C T_1 values that do not appear to be sufficiently long to allow their use as MRI probes, while the introduction of the spacer in **7** is effective in lengthening the ^{13}C carbonyl T_1 of the corresponding alkene **7a** up to 21.0 s at 9.37 T.

As shown by **7a** uptake experiments on human myelogenous leukemia cells, the glucose moiety drives the cellular internalization of the probe, which can be observed even at low incubation times, thus reporting on the activity of glucose transporters that are usually up-regulated in tumor cells. Thus, the selective accumulation of this hyperpolarized molecule may act as a sensitive biomarker of the tumor staging, and it may provide interesting insights for designing MRI alternatives to FDG/PET-based procedures.

Experimental Section

NMR spectra were recorded on a Bruker Avance600 spectrometer, operating at 600 MHz for ^1H, 150 MHz for ^{13}C, and 243 MHz for ^{31}P, and on a JEOL EX-400 spectrometer operating at 400 MHz for ^1H. For para-H_2 experiments, single-scan spectra were acquired. T_1 measurements were carried out on ^{13}C-enriched compounds by using the inversion recovery pulse sequence.

Mass spectra were recorded on a Waters Micromass ZQ instrument equipped with ESCi source.

Solvents were stored over molecular sieves and purged with nitrogen before use. Hydrogen was produced by a CLAIND generator, model HG300.

Para-enriched hydrogen (52%) was prepared by storing H_2 over Fe_2O_3 at 77 K for 1 h.

Para-hydrogenation reactions were carried out in ALTADENA[23] conditions in a 5 mm NMR tube equipped with a Young valve.

(42) Macheda, M. I.; Rogers, S.; Best, J. D. *J. Cell. Physiol.* **2005**, *202*, 6546.
(43) Rodríguez-Enríquez, S.; Marín-Hernández, A.; Gallardo-Pérez, J. C.; Moreno-Sánchez, R. *J. Cell Physiol* **2009**, *221*, 552.
(44) Harris, T.; Eliyahu, G.; Frydman, L.; Degani, H. *Proc. Natl. Acad. Sci. U.S.A.* **2009**, *106*, 18131.
(45) van Heeswijk, R. B.; Morgenthaler, F. D.; Gruetter, R. *Magn. Reson. Imag.* **2007**, *25*, 821.
(46) Gabellieri, C.; Leach, M. O.; Eykyn, T. R. *Contrast Media Mol. Imaging* **2009**, *4*, 143.

[Bis(diphenylphosphino)butane](1,5-cyclooctadiene)rhodium(I) tetrafluoroborate (4 mg) was dissolved in an acetone-d_6/CD_3OD 9:1 mixture or in pure acetone-d_6 (0.4 mL) and activated by reaction with H_2. Normal H_2 was then replaced by the para-H_2-enriched mixture (4 atm) after addition of the substrate (0.015 mmol for ^{1}H NMR spectra or 0.05 mmol for ^{13}C NMR spectra). The hydrogenation was carried out by shaking the tube for 10 s.

The magnetic field cycle was pursued by quickly inserting the tube into a μ-metal shield (field strength 0.1 μT) and then slowly removing the shield (the entire field-cycling procedure required 3−5 s).

Cell Culture, Toxicity Assays, and Uptake Experiments. K562 (human myelogenous leukemia) cells were grown in 75 cm^2 flasks in RPMI medium supplemented with 5% fetal bovine serum, 2 mM glutamine, 100 IU/mL penicillin, and 100 μg/mL streptomycin in a humidified incubator at 37 °C and at CO_2/air (5:95 v/v).

For toxicity tests, cell lines were seeded (~2 × 10^6/dish) in 6 cm diameter Petri dishes with 2 mL of the appropriate medium supplemented with fetal bovine serum, 2 mM glutamine, 100 IU/mL penicillin, and 100 μg/mL streptomycin. Cells were incubated in the presence of 100 mM **7a** at 37 °C and at CO_2/air (5:95 v/v) for 4 h. The trypan-blue exclusion test was used to assess cell viability. Viability is expressed in % (ratio of viable cells to total cells × 100).

For uptake experiments, K562 cells were seeded (~20 × 10^6/dish) in 6 cm diameter Petri dishes as described above and incubated in the presence of 100 mM **7a** at 37 °C, 5% CO_2 for 1, 5, 10, 60, and 240 min, and at 4 °C for 60 min. At the end of the incubation, the medium was removed, and cells were washed three times with phosphate-buffered saline. Cells were harvested in 500 μL of H_2O/D_2O and lysated by sonication. ^{13}C spectra were acquired on cell lysates. [1-^{13}C]glucose (50 mM) was added as internal standard in order to obtain a quantitative assessment of the cellular uptake.

Phosphorylation Assay. To assess phosphorylation of **7a**, a commercial enzymatic glucose assay kit (Sigma Aldrich) was used. The kit is designed for the enzymatic quantification of glucose in food and other materials. Glucose is phosphorylated by adenosine triphosphate (ATP) in the reaction catalyzed by hexokinase. Glucose-6-phosphate (G6P) is then oxidized to 6-phospho-gluconate in the presence of oxidized nicotinamide adenine dinucleotide (NAD) in a reaction catalyzed by glucose-6-phosphate dehydrogenase (G6PDH). During this oxidation, an equimolar amount of NAD is reduced to NADH. The consequent increase in absorbance at 340 nm is directly proportional to glucose concentration. **7a**, however, can undergo only the phosphorylation step but not the subsequent oxidation. Therefore, ^{31}P 1D-NMR experiments on the kit mixture were acquired to assess the presence of the phosphorylated form of **7a**. The absence of any signal attributable to a phosphorylated/oxidized product indicates that phosphorylation did not occur. The same reaction assay performed on glucose was used as a reference. Both compounds were used at a concentration of 10 mM in the reaction kit (final volume 500 μL, H_2O/D_2O 90:10). ^{31}P 1D-NMR spectra were collected with a recycle delay d1 = 2 s, number of scans ns = 2048, excitation pulse p1 = 90°, for a total experimental time of 59 min.

The same test was used to assess the phosphorylation/oxidation of **5a**, which, at variance with **7a**, can undergo both reactions. The assay is indeed designed so that the phosphorylated compound is quantitatively oxidized. Since in this case the test was positive, as verified by UV measurements on unlabeled **5a**, it was repeated with the ^{13}C-enriched derivative, and the ^{13}C NMR spectrum of the mixture was recorded in order to determine the ^{13}C shift between the starting compound **5a** and the corresponding phosphorylated and oxidized form.

Synthesis of Substrates. 1,3,4,6-Tetra-*O*-acetyl-2-(but-2-ynylamido)-2-deoxy-α,β-D-glucopyranose (2). A solution of 2-butynoic acid chloride was prepared by means of addition of 1-chloro-*N*,*N*,2-trimethylprop-1-en-1-amine (400 μL, 3.0 mmol) to a cooled solution (−50 °C) of acid (3.0 mmol) in anhydrous dichloromethane (4 mL). The resulting mixture was kept 4 h at −30 °C and then added slowly to a cooled solution (−30 °C) of 1,3,4,6-tetra-*O*-acetyl-β-D-glucosamine hydrochloride (900 mg, 2.3 mmol) and ethyldiisopropylamine (920 μL, 5.3 mmol) in dichloromethane (12 mL). The mixture was allowed to reach 0 °C, and then the reaction was quenched by addition of water. The mixture was shaken with aqueous HCl (5%, 10 mL) then $NaHCO_3$ (5%, 10 mL) and water (10 mL). The dichloromethane extract was dried (Na_2SO_4) and evaporated. The product was crystallized from the liquid residue by addition of ether and petroleum ether. Yield: 820 mg (85%). ^{1}H NMR (α anomer, CD_3OD): δ 5.79 (d, H-1), 5.30 (dd, H-3), 5.05 (dd, H-4), 4.31 (dd, H-6), 4.13 (2dd, H-6′ + H-2), 3.95 (m, H-5), 2.12 (s, $OCOCH_3$), 2.08 (s, $OCOCH_3$), 2.04 (s, $OCOCH_3$), 2.03 (s, $OCOCH_3$), 1.99 (s, CH_3). ^{13}C{^{1}H} NMR (α anomer, CD_3OD): δ 172.27, 171.58, 171.19, 170.53 (acetylic CO groups), 155.91 (butynoyl CO group), 93.07 (C-1), 86.15 and 74.78 (C≡C), 73.72 (C-5), 73.55 (C-3), 69.64 (C-4), 62.86 (C-6), 54.12 (C-2), 20.57 (3C), 20.50 (1C, acetylic CH_3), 3.06 (butynoic CH_3). MS: calcd for $C_{18}H_{23}NO_{10}$ (MW + H^+ − $OCOCH_3$) 354.12, found 354.41.

2-(But-2-ynylamido)-2-deoxy-α,β-D-glucopyranose (1). Compound **2** was deacetylated in sodium methanolate−methanol (0.1 M, 5 mL) in 1 h. The mixture was then neutralized with Dowex 50 (H^+), the resin was filtered off and washed with methanol, and the combined filtrates were evaporated. The crude viscous product was separated by chromatography on a cellulose column (2 × 15 cm) in *n*-butanol−water (10:1) as a mobile phase. Yield (from **2**): 150 mg (63%) of hygroscopic crystals. ^{1}H NMR (α anomer, CD_3OD): δ 5.13 (d, H-1), 3.89 (dd, H-2), 3.70−3.87 (overlapping signals from H-3, H-4, and H-6), 3.39 (m, H-5), 2.00 (s, CH_3). ^{13}C{^{1}H} NMR (α anomer, CD_3OD): δ 156.15 (CO), 92.25 (C-1), 85.56 and 75.28 (C≡C), 73.05 and 72.32 (C-3 and C-4), 72.22 (C-5), 62.69 (C-6), 56.17 (C-2), 3.19 (CH_3). MS: calcd for $C_{10}H_{15}NO_6$ (MW + H^+) 246.09, found 246.40; (MW + H^+ − H_2O) 228.08, found 228.34; (MW + H^+ − 2H_2O) 210.07, found 210.35; (MW + Na^+) 268.08, found 268.36.

2-(propiolamido)-2-deoxy-α,β-D-glucopyranose (3). The same 3.0 mmol scale procedure described for **2**, using 3-(trimethylsilyl)-propynoic acid in place of 2-butynoic acid, was used for preparation of 2-[3-(trimethylsilyl)propiolamido]-2-deoxy-α,β-D-glucopyranose (yield 900 mg, 81%). The obtained trimethylsilyl derivative (470 mg, 1.0 mmol) and K_2CO_3 (150 mg 1.1 mmol) in anhydrous methanol (20 mL) were stirred for 3 h at room temperature. The solution was then neutralized with Dowex 50 (H^+), the resin was filtered off and washed with methanol, and the combined filtrates were evaporated. The crude syrupy product was purified by chromatography on a cellulose column (2 × 15 cm) in *n*-butanol−water (10:1) as a mobile phase. Yield: 140 mg (61%). ^{1}H NMR (α anomer, CD_3OD): δ 5.17 (d, H-1), 3.92 (dd, H-2), 3.85 (overlapping signals from H-3 and H-4), 3.77 (dd, 2H, H-6), 3.65 (s, ≡CH, this signal disappears after 1 h in CD_3OD), 3.41 (dd, H-5). ^{13}C{^{1}H} NMR (α anomer, CD_3OD): δ 154.96 (CO), 92.19 (C-1), 77.82 (−C≡), 76.06 (≡CH, this signal shows a $^1J_{^{13}C,^2D}$ = 40.0 Hz (t) after 1 h in CD_3OD), 73.08 (C-3 or C-4), 72.38 (C-5), 72.19 (C-4 or C-3), 62.73 (C-6), 56.28 (C-2). MS: calculated for $C_9H_{13}NO_6$ (MW + H^+) 232.07, found 232.40; (MW + H^+ − H_2O) 214.06, found 214.38; (MW + H^+ − 2H_2O) 196.05, found 196.36; (MW + Na^+) 254.06, found 254.35.

6-*O*-(But-2-ynoyl)-α,β-D-glucopyranose (4) and 2-*O*-(But-2-ynoyl)-α,β-D-glucopyranose (5). A solution of butynoyl chloride was prepared by means of addition of 1-chloro-*N*,*N*,2-trimethylprop-1-en-1-amine (0.93 mL, 7.0 mmol) to a cooled solution (−50 °C) of butynoic acid (590 mg, 7.0 mmol) in anhydrous THF (3 mL) under an inert atmosphere. The mixture was kept 4 h at −30 °C. Finely powdered D-glucose (1.25 g, 6.9 mmol) was in the meantime dissolved in anhydrous DMF (20 mL) by means of heating in a hot bath (80 °C) while stirring. Everything was kept under an inert atmosphere. The resulting solution was cooled, and then K_2CO_3 (5 μm powder, 1.44 g, 10.3 mmol) and 4-Å molecular sieves (5 μm)

were added. The mixture was cooled using an ice−water bath. The pre-prepared solution of butynoyl chloride was slowly added to the glucose solution. The reaction mixture was stirred overnight at room temperature. Solvents were then evaporated *in vacuo* at 45 °C. The syrupy residue was prepurified on a short silica gel column (3 × 7 cm) using 4% MeOH in EtOAc for elution. Crude product was purified by chromatography on a silica gel column (30 g) in MeOH−EtOAc (1:30) as a mobile phase. Fractions containing **4** ($R_f \approx 0.25$) or **5** ($R_f \approx 0.3$) were collected and evaporated, and the residues were crystallized from EtOH−Et_2O. Yield: 110 mg (6.4%) of **4** and 20 mg of **5** (1.2%). ^{1}H NMR for **4** (CD_3OD): δ 5.12 (d, H-1α), 4.51 (d, H-1*β*), 4.45 (dd, H-6*β*), 4.27 (dd, H-6α), 4.00 (m, H-5α), 3.70 (dd, H-3α), 3.52 (m, H-5*β*), 3.38−3.30 (overlapping signals from H-3*β*, H-2α, H-4α and H-4*β*), 3.17 (dd, H-2*β*), 2.03 (CH_3). ^{13}C{^{1}H} NMR for **4** (CD_3OD): δ 155.06 (COα), 154.95 (CO*β*), 98.21 (C-1*β*), 93.97 (C-1α), 86.97 (−C≡*β*), 86.91 (−C≡α), 77.87 (C-3*β*), 76.13 (C-2*β*), 75.03 (C-5*β*), 74.73 (C-3α), 73.70 (C-2α), 72.87 (≡C-α), 72.81 (≡C-*β*), 71.83 (C-4α), 71.59 (C-4*β*), 70.37 (C-5α), 66.00 (C-6α), 65.91 (C-6*β*), 3.04 (CH_3). ^{1}H NMR for **5** (CD_3OD): δ 5.29 (d, H-1α), 4.71 (dd, H-2*β*), 4.67 (d, H-1*β*), 4.62 (dd, H-2α), 3.90 (dd, H-4α), 3.82 (d, H-6α), 3.71 (d, H-6*β*), 3.54 (dd, H-3*β*), 3.38−3.33 (overlapping signals from H-3α, H-5α, H-4*β*, and H-5*β*), 2.04 (CH_3). ^{13}C{^{1}H} NMR for **5** (CD_3OD): δ 154.78 (COα), 154.55 (CO*β*), 96.00 (C-1*β*), 90.83 (C-1α), 87.68 (−C≡α), 87.65 (−C≡*β*), 78.10 (C-5*β*), 77.79 (C-2*β*), 76.64 (C-2α), 75.84 (C-3*β*), 72.95 (≡C-α+*β*), 72.84 (C-5α), 71.87 (C-3α), 71.77 (C-4α), 71.63 (C-4*β*), 62.58 (C-6*β*), 62.43 (C-6α), 3.15 (CH_3). MS: calcd for $C_{10}H_{14}O_7$ (MW + H^+ − H_2O) 229.06, found 229.40 for **4** and 229.41 for **5**; (MW + H^+ − $2H_2O$) 211.05, found 211.33 for **4** and 211.38 for **5**; (MW + Na^+) 269.06, found 269.34 for **4** and 269.39 for **5**.

1-*O*-(But-2-ynoyl)-α,*β*-D-glucopyranose (6). A 0.27 g sample of D-glucose (1.5 mmol) was dissolved in about 5 mL of anhydrous DMF under Ar atmosphere. Next, 0.176 g of butynoic acid (1.98 mmol) and 0.559 g of triphenylphosphine (2.31 mmol) were added to the solution, and then 0.410 mL of diisopropyl azodicarboxylate (DIAD) (2.31 mmol) was slowly dropped into the solution at 0 °C. The mixture was then warmed to room temperature and stirred under an Ar atmosphere for 24 h. The solvent was removed and the product purified by column chromatography on silica gel, using dichloromethane−methanol from 95:5 to 85:15 for elution. The obtained isomers **5** and **6** were then separated by column chromatography on silica gel using EtOAc−MeOH 98:2 for elution. Yield: 0.25 g of pure **6**, 66.7%. ^{1}H NMR (CD_3OD): δ 6.19 (d, H-1α), 5.52 (d, H-1*β*), 3.83 (dd, H-6α), 3.75−3.69 (H-3α and H-6*β*, overlapping), 3.63−3.60 (H-2α and H-5α, overlapping), 3.48−3.35 (H-2*β*, H-3*β*, H-4α, H-4*β*, and H-5*β*, overlapping), 2.06 (CH_3). ^{13}C{^{1}H} NMR (CD_3OD): δ 153.97 (COα), 153.74 (CO*β*), 96.57 (C-1*β*), 94.96 (C-1α), 89.26 (−C≡*β*), 88.75 (−C≡α), 78.90 (C-5*β*), 77.89 (C-3*β*), 76.41 (C-5α), 74.74 (C-3α), 73.80 (C-2*β*), 72.87 (≡C-α), 72.74 (≡C-*β*), 72.10 (C-2α), 70.95 (C-4*β*), 70.87 (C-4α), 62.34 (C-6*β*), 62.28 (C-6α), 3.52 (CH_3). MS: calcd for $C_{10}H_{14}O_7$ (MW + H^+ − H_2O) 229.06, found 229.30; (MW + H^+ − $2H_2O$) 211.05, found 211.21; (MW + Na^+) 269.06, found 269.25.

1-*O*-[2-(But-2-ynoyl)ethyl]-α,*β*-D-glucopyranose (7). A 0.25 g sample of 1-*O*-(D-glucopyranosyl)ethylene glycol, prepared according to ref 47 (1.15 mmol), was dissolved in about 5 mL of anhydrous DMF under an Ar atmosphere. Next, 0.133 g of butynoic acid (1.561 mmol) and 0.439 g of triphenylphosphine (1.672 mmol) were added to the solution, and then 0.324 mL of DIAD (1.672 mmol) was slowly dropped into the solution at 0 °C. The mixture was then warmed to room temperature and stirred under an Ar atmosphere for 24 h. The solvent was removed and the product purified by column chromatography on silica gel, using dichloromethane−methanol from 95:5 to 85:15 for elution. Yield: 90.0 mg, 28.7%. ^{1}H NMR (α anomer, CD_3OD): δ 4.87 (H-1), 4.35 (m, CH_2, H-8), 3.94 (m, CH_2, H-7), 3.81 (dd, H-4), 3.80−3.65 (overlapping signals for H-5 and H-6), 3.45 (dd, H-2), 3.36 (dd, H-3), 2.04 (CH_3). ^{13}C{^{1}H} NMR (α anomer, CD_3OD): δ 155.23 (CO), 100.62 (C-1), 87.53 (−C≡), 75.09 (C-4), 73.88 (C-5), 73.55 (C-2), 73.11 (≡C−), 71.60 (C-3), 67.02 (CH_2, C-7), 66.12 (CH_2, C-8), 62.59 (C-6), 3.45 (CH_3). MS: calcd for $C_{12}H_{18}O_8$ (MW + H^+ − H_2O) 273.10, found 273.03; (MW + Na^+) 313.09, found 313.24.

^{13}C-Enriched 4, 6, and 7. ^{13}C-enriched derivatives were prepared as reported above, by using ^{13}C-enriched butynoic acid.

^{13}C-Enriched Butynoic Acid. A 1.0 g (41.7 mmol) sample of sodium hydride was suspended in 50 mL of anhydrous dimethylsulfoxide under an inert atmosphere and heated at 75 °C until the end of gas evolution. The mixture was then cooled at room temperature and a few milligrams of triphenylmethane added; the solution turned red. Propyne was fluxed into the solution until the color turned to white. After filtration, the solid was resuspended in anhydrous THF and transferred to another flask, equipped with a manometer and a $^{13}CO_2$ inlet. $^{13}CO_2$ was introduced into the flask, and the mixture was stirred vigorously until the gas consumption ceased. The suspension was filtered, the solid was washed with Et_2O, dried in vacuum, and then dissolved in water, and 3.5 mL of HCl (37%) was added dropwise at 5 °C. The solution was extracted with Et_2O (5 × 25 mL). The organic phase was dried over $MgSO_4$ and evaporated. [^{13}C]Butynoic acid was crystallized from EtOAc−petroleum ether. Yield: 2.5 g (70%). ^{1}H NMR (acetone-d_6): δ 2.09 (d, $J_{^{13}C,^1H}$ = 1.6 Hz). ^{13}C{^{1}H} NMR (acetone-d_6): δ 153.82 (CO), 84.99 ($J_{^{13}C,^{13}C}$ = 19.2 Hz, C≡C), 72.75 ($J_{^{13}C,^{13}C}$ = 121.5 Hz, C≡C), 2.47 (CH_3).

1-*O*-[2-(*cis*-But-2-enoyl)ethyl]-α,*β*-D-glucopyranose (7a). 7a for uptake experiments was prepared by homogeneous catalytic hydrogenation of **7** in CD_3OD solution, following the reaction by ^{1}H NMR. After reaction completion, the catalyst was removed by column chromatography on silica gel, using dichloromethane−methanol from 95:5 to 85:15 for elution. ^{1}H NMR (α anomer, CD_3OD): δ 6.46 (=CH), 5.88 (HC=), 4.89 (H-1), 4.36 (m, CH_2, H-8), 3.99 (m, CH_2, H-7), 3.90−3.65 (overlapping signals for H-4, H-5, and H-6), 3.46 (dd, H-2), 3.36 (dd, H-3), 2.20 (d, CH_3). ^{13}C{^{1}H} NMR (α anomer, CD_3OD): δ 167.78 (CO), 146.85 (=CH), 121.11 (HC=), 100.32 (C-1), 74.88 (C-4), 73.63 (C-5), 73.35 (C-2), 71.45 (C-3), 67.05 (CH_2, C-7), 64.02 (CH_2, C-8), 62.64 (C-6), 15.63 (CH_3).

Acknowledgment. We gratefully acknowledge discussion with Prof. D. Canet. Dr. Luca Biondi (Bracco Imaging S.p.A., Colleretto Giacosa, Italy) is also acknowledged for acquisition of NMR spectra on cell lysates. This work has been carried out in the frame of the EU-NEST STREP project (n. 005032). Support from MIUR (Firb project n. RBIP06293N) and Regione Piemonte (POR FESR 2007/2013, line I.1.1) is acknowledged.

Supporting Information Available: ^{1}H, ^{13}C, ^{13}C-DEPT135, HMBC, and HMQC spectra of **1**, **2**, and **3**; ^{1}H, ^{13}C, HMBC, HMQC, ^{1}H COSY NMR spectra of **4** and **5**; ^{1}H, ^{13}C, ^{13}C-DEPT135, HMBC, HMQC, and ^{1}H COSY spectra of **6** and **7**; ^{13}C NMR spectra of cell lysates after 1 h incubation with **7a** at 37 and 4 °C. This material is available free of charge via the Internet at http://pubs.acs.org.

JA101399Q

(47) Vallinayagam, R.; Schmitt, F.; Barge, J.; Wagnieres, G.; Virginie Wenger, V.; Neier, R.; Juillerat-Jeanneret, L. *Bioconjugate Chem.* **2008**, *19*, 821.